

Computing with Curvelets: From Image Processing to Turbulent Flows

JIANWEI MA^{1,3} AND GERLIND PLONKA²

¹ School of Aerospace, Tsinghua University, Beijing 100084, China

² Department of Mathematics, University of Duisburg-Essen, 47048 Duisburg, Germany

³ Centre de Geosciences, Ecole des Mines de Paris, 77305 Fontainebleau Cedex, France

Abstract

The curvelet transform is a multiscale and multidirectional transform, which allows an almost optimal non-adaptive sparse representation for curve-like features and edges. Applications of curvelets have quicken increasing interest in the community of applied mathematics, signal processing and seismic geology over the past years. In this paper, we describe some recent applications involving image processing, seismic data exploration, turbulent flows, and compressed sensing.

1 INTRODUCTION

Most natural images/signals exhibit line-like edges, i.e., discontinuities across curves (so-called line or curve singularities). Although applications of wavelets have become increasingly popular in scientific and engineering fields, traditional wavelets perform well only at representing point singularities, since they ignore the geometric properties of structures and do not exploit the regularity of edges. Therefore, wavelet-based compression, denoising, or structure extraction become computationally inefficient for geometric features with line and surface singularities. For example, when we download compressed images or videos, we often find a mosaic phenomenon (i.e., block artifacts along edges of the images). This mosaic phenomenon mainly results from the poor ability of wavelets to handle line singularities.

A multiresolution geometric analysis, named curvelet transform was proposed [2, 4, 5] in order to improve the drawback of conventional two-dimensional (2D) discrete wavelet transforms. Curvelets form an effective model that not only considers a multiscale time-frequency local partition, but also makes use of the direction of geometric features. In the 2D case, the curvelet transform allows an almost optimal sparse representation of objects with C^2 -singularities. Unlike the isotropic elements of wavelets, the needle-shaped elements of this transform possess very high directional sensitivity and anisotropy (see Fig. 1 for the 2D case). Such an element is very efficient in representing line-like edges. Excellent performance of the curvelet transform has been shown in fields of image processing, see e.g. [21, 22, 26, 30].

Recently, the curvelet transform has been extended to 3D by Ying et al. [2, 33]. Figure 2 shows a 3D curvelet element. Observe that in the spatial domain, the elements are of plate-like shape, they are smooth within the plate but exhibit oscillating decay in the normal direction of the plate.

The Fourier transform is a global method. One needs lots of terms to reconstruct a discontinuous function. A lack of terms leads to Gibbs oscillation phenomenon. Wavelets, because they are localized and possess multiscale properties, can sparsely represent signals in 1D (i.e., one can use a limited number of terms to reconstruct the signals with good accuracy). Curvelets, combining ideas of geometry and multiscale analysis, can sparsely represent higher-dimensional singularities (e.g., edges and surfaces) effectively.

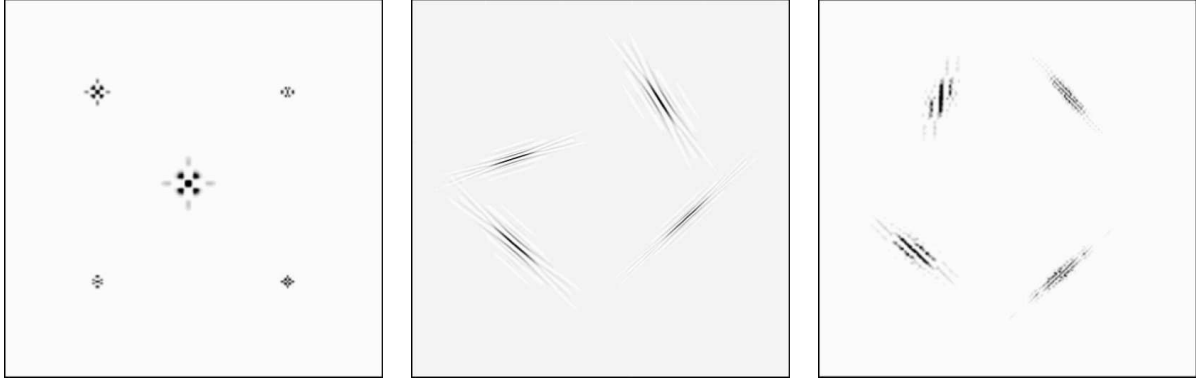


Figure 1: The elements of wavelets (left), curvelets (middle) and contourlets (right) in time domain.

2 BRIEF HISTORY

Over the past two decades, after the great work by Meyer, Daubechies, Mallat, etc., wavelets have established an impressive reputation as a tool for mathematical analysis and signal processing. But, the poor directionality of discrete wavelet transform (DWT) has undermined its further usage in many applications. Significant progress in the development of directional wavelets has been made in recent years. The complex wavelet transform is one way to improve directional selectivity and only requires $\mathcal{O}(N)$ computational cost. However, the complex wavelet transform has not been widely used in the past, due to the difficulty in designing complex wavelets with perfect reconstruction properties and good filter characteristics. One popular technique is the dual-tree complex wavelet transform (DT CWT) proposed by Kingsbury [20], which added perfect reconstruction to the other attractive properties of complex wavelets, including approximate shift invariance, six directional selectivities, limited redundancy and efficient $\mathcal{O}(N)$ computation.

The directional selectivity (six directions) is much better than classical DWT (three directions), but it is still limited.

In 1999, an anisotropic geometric wavelet, named ridgelet, was proposed by Candès and Donoho [3]. The ridgelet transform is optimal at representing straight-line singularities. The transform with arbitrary directional selectivity provides a key to the analysis of higher dimensional singularities. The main drawback of the ridgelet transform is the limitation of its applicability to objects with global straight-line singularities, which is rarely the case in real applications [24]. In order to analyze local line or curve singularities, a natural idea is to consider a block partition for the images, and then to apply the ridgelet transform to the partitioned sub-images. This block ridgelet based transform, which is named curvelet transform, was first proposed by Candès and Donoho in 2000, see [4]. Apart from the blocking effects, however, the application of this so-called first-generation curvelet transform is limited because the geometry of ridgelets is itself unclear, as they are not true ridge functions in digital images. Later, a considerably simpler second-generation curvelet transform based on a frequency partition technique was proposed by the same authors, see [5].

It should be noted that several other directional multi-resolution bases, such as wedgelets [13], bandlets [28], contourlets [11], shearlets [16], platelets [32], have been proposed independently to identify and restore geometric features. These geometric/directional wavelets are uniformly

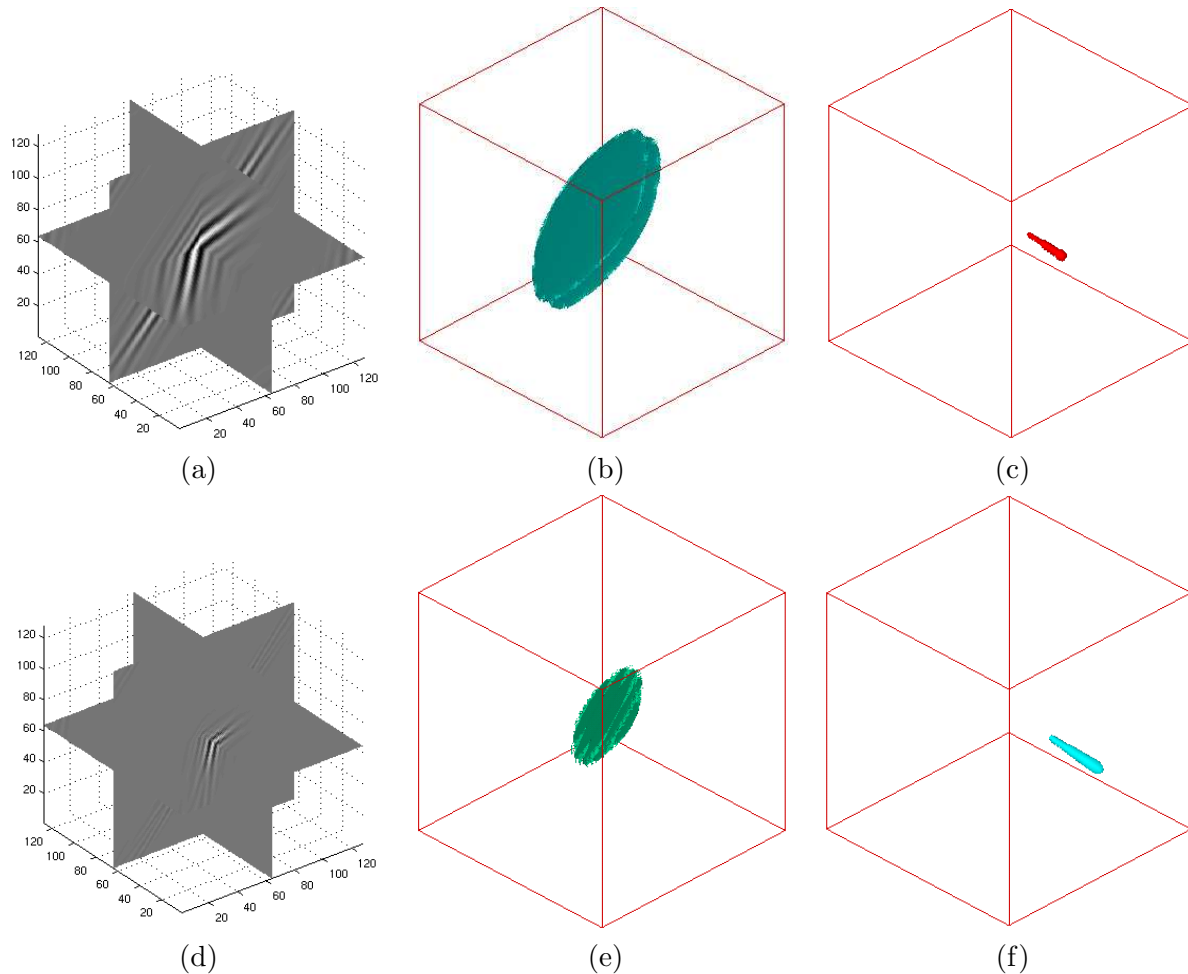


Figure 2: An element of 3D curvelets at a coarser scale (upper row) and finer scale (lower row) is shown in three cross-sections (left column) and isosurface (middle column). The right column shows their frequency support.

called X-lets.

In particular, the directional-filter-bank based contourlet transform [11] can be seen as a certain discrete form of the curvelet transform. For contourlets, there exists an orthogonal version that is faster than current discrete curvelet algorithms [2]. But contourlet functions have less clear directional features than curvelets (see Fig. 1), which leads to artifacts in denoising and compression.

3 PROPERTIES OF CURVELET FUNCTIONS

Let us briefly recall the main features of curvelet functions that admit their wide range of applications in different fields.

Curvelets have a compact support in frequency domain. This support is a polar wedge or a trapezoid. The wedges are rotated around zero, such that the supports of all curvelets represent

a tiling of the two-dimensional frequency domain.

Curvelet functions $\phi_{j,k,l}$ are usually indicated by three indices; j denotes the scale index, l the orientation index, and $k \in \mathbb{Z}^2$ the location in time domain. In Figure 3, we have illustrated some supports of curvelet functions in frequency domain. The scale j denotes the distance 2^j of the support wedge from zero and the length 2^{j+1} as well as the width $2^{j/2}$ of the polar wedge. The orientation l determines the rotation angle $2^{-\lceil j/2 \rceil} \pi l / 2 \in [0, 2\pi)$ of the wedge, where $l = 0, \dots, 4 \cdot 2^{\lceil j/2 \rceil} - 1$. Finally, the location $(k_1/2^j, k_2/2^{j/2})$ with $k = (k_1, k_2) \in \mathbb{Z}^2$ indicates the translation of the curvelet function in time domain.

As one can see from Figure 3, the wedges are longer and thinner with growing j . Correspondingly in time domain, curvelets have a well-localized needle-shaped form, see Figure 1 (middle).

The main properties of curvelets can be summarized as follows.

1. The family of curvelet functions forms a tight frame of $L_2(\mathbb{R}^2)$. That means, each function $f \in L_2(\mathbb{R}^2)$ has a representation

$$f = \sum_{j,k,l} \langle f, \phi_{j,k,l} \rangle \phi_{j,k,l},$$

where $\langle f, \phi_{j,k,l} \rangle$ denotes the L_2 -scalar product of f and $\phi_{j,k,l}$. The coefficients $c_{j,k,l} := \langle f, \phi_{j,k,l} \rangle$ are called **curvelet coefficients**.

2. The transform

$$Tf := (c_{j,k,l})_{j,k,l},$$

that computes the sequence of curvelet coefficients from $f \in L_2(\mathbb{R}^2)$, is called **curvelet transform**. A fast curvelet transform can be realized by computing first the Fourier transform of f (by an FFT-algorithm), and computing the scalar product $\langle \hat{f}, \hat{\phi}_{j,k,l} \rangle$ in frequency domain, using the small compact support of $\hat{\phi}_{j,k,l}$, see [2].

3. Curvelets are well-localized in time- and frequency domain. Because of their shape, they possess a high directional sensitivity.
4. Curvelets are constructed by tiling of the frequency plane, they are complex functions. One can construct also real curvelet functions by adding two curvelets that are supported in frequency domain on two polar wedges being symmetric with respect to zero.
5. Curvelets possess an infinite number of directional moments. This property implies that, if the essential support of the curvelet $\phi_{j,k,l}$ lies in a smooth part of f , then the corresponding curvelet coefficient $c_{j,k,l}$ will be small, while, if the essential support of $\phi_{j,k,l}$ is aligned with an edge of f , then $c_{j,k,l}$ will be significant.

These properties of the curvelet frame are essential for its ability to detect wave front sets efficiently.

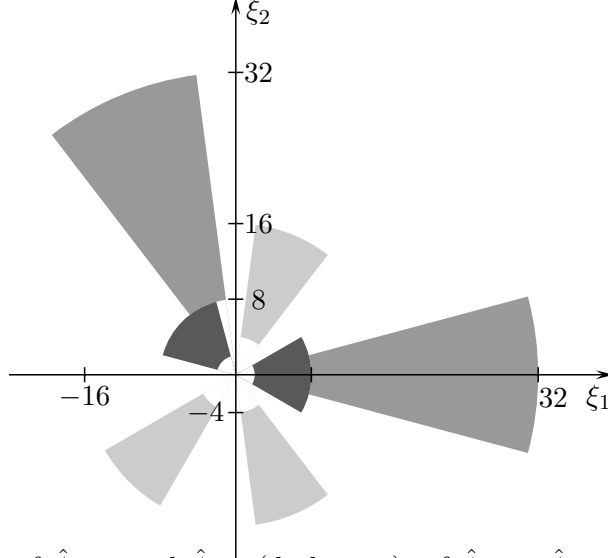


Figure 3: Maximal supports of $\hat{\phi}_{2,k,0}$ and $\hat{\phi}_{2,k,5}$ (dark grey); of $\hat{\phi}_{3,k,3}$, $\hat{\phi}_{3,k,6}$ and $\hat{\phi}_{3,k,13}$ (light grey); and of $\hat{\phi}_{4,k,0}$ and $\hat{\phi}_{4,k,11}$ (grey).

4 CURVELET SHRINKAGE

The shrinkage/thresholding plays a key role in applications of curvelets. We take the curvelet shrinkage as

$$P_\sigma u = T^{-1} S_\sigma T(u),$$

where T denotes the curvelet transform, T^{-1} the inverse transform, and S_σ is a thresholding function. Hence, a curvelet shrinkage consists of three steps. First, we apply a forward curvelet transform. Secondly, we remove some insignificant curvelet coefficients by using a thresholding function in curvelet domain. Finally, we apply the inverse curvelet transform in order to reconstruct a function from the remaining significant curvelet coefficients. Here, how to choose the threshold function S_σ is critical. In general, it can be taken as a soft thresholding function defined by a fixed threshold $\sigma > 0$,

$$S_\sigma(x) = \begin{cases} x - \sigma, & x \geq \sigma, \\ 0, & |x| < \sigma, \\ x + \sigma, & x \leq -\sigma, \end{cases}$$

or a hard thresholding function,

$$S_\sigma(x) = \begin{cases} x, & |x| \geq \sigma, \\ 0, & |x| < \sigma, \end{cases}$$

or a continuous garrote thresholding,

$$S_\sigma(x) = \begin{cases} x - \frac{\sigma^2}{x}, & |x| \geq \sigma, \\ 0, & |x| < \sigma, \end{cases}$$

which may be a good choice since large coefficients nearly remain unaltered. These simple thresholding functions are easy to implement in engineering fields. However, as wavelets, the curvelet shrinkage also suffers from pseudo-Gibbs oscillating artifacts.

In [21], a total variation (TV)-constraint curvelet shrinkage was proposed in order to reduce these artifacts (see also [24]). For a function u with $|\nabla u| \in L^1(\Omega)$, the total variation functional is defined by

$$TV(u) := \int_{\Omega} |\nabla u(x)| dx,$$

where $|\nabla u(x, y)| := (u_x(x, y) + u_y(x, y))^{1/2}$ denotes the Euclidean norm of the partial derivatives of u . The idea of TV constraint curvelet shrinkage is as follows. Instead of setting the set of insignificant curvelet coefficients to zero as it is done with conventional shrinkage, one tries to find optimal small values for these coefficients such that the total variation $TV(u)$ is minimized, and the pseudo-Gibbs artifacts are removed. Using a reconstructed image after curvelet thresholding u_c as an initial guess, the TV-constraint shrinkage can be computed by a projected subgradient descent scheme

$$u^{l+1} = u^l - t_l P_V(g_{TV}(u^l)). \quad (1)$$

Here $g_{TV}(u)$ denotes the subgradient of TV at u . The step size t_l can be taken appropriately to ensure convergence. $P_V(u)$ denotes a projection of u on a constrained subspace V . That means, only the coefficients with absolute value smaller than a given threshold σ will be changed by the iterative process. We have $P_V(u) = T^{-1} \tau^{-1} T(u)$ where the τ^{-1} denotes a so-called inverse thresholding function,

$$\tau^{-1}(x) := \begin{cases} 0, & x \geq \sigma, \\ x, & x < \sigma. \end{cases}$$

Fig. 4 shows a comparison of image denoising by Daubechies DB4 wavelet shrinkage, contourlet shrinkage, curvelet shrinkage, and the TV-constraint curvelet shrinkage with 25 iterations. The elapsed computation time for the four methods is 1.10s, 1.25s, 1.27s, and 23.11s using a laptop with Intel Pentium processor 1.86 GHz and 512 MB memory, respectively. It can be seen that the TV-constraint curvelet shrinkage leads to a promising gain at the expenses of computation time.

5 RECENT APPLICATIONS

In this section, we shall review applications of the curvelets in image processing, seismic exploration, turbulent flows, and compressed sensing, to show their potential to upstage the wavelet transforms to some extent.

5.1 Image processing

Digital images are 2D matrices. The so-called image processing is to adjust the values of matrices in order to get clear features. The adjusting of values should obey a certain mathematical model. One main challenge in image processing is how to build suitable mathematical models for practical requirements. Taking denoising as example, there exist four classical models: frequency analysis, statistical analysis, PDE diffusion, and variational methods. In frequency analysis, one assumes that components with high frequency are interpreted as noise to be removed while those with low frequency are seen as features to be remained. A crucial problem in denoising is to keep sharp structures when one removes noise. The sharp edges also consist of high-frequency components, thus they are often smoothed out since they can not be distinguished from noise.

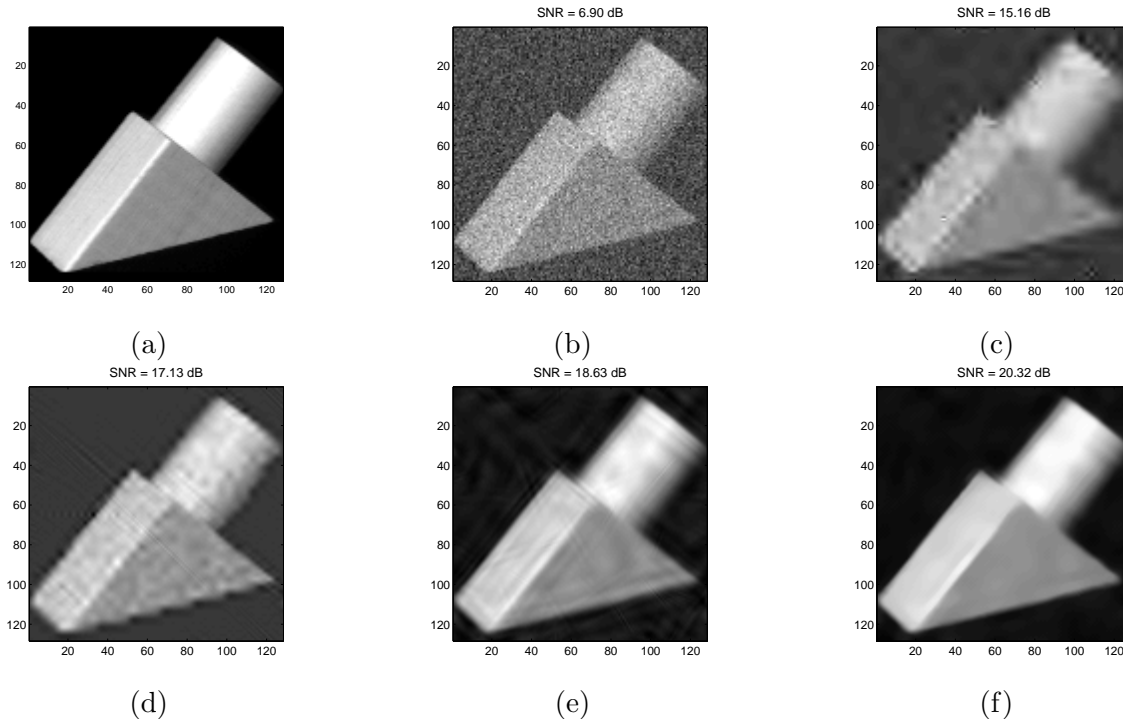


Figure 4: Image denoising. (a) original object. (b) noisy object. (c) wavelet denoising. (d) contourlet denoising. (e) curvelet denoising by hard thresholding. (f) TV-curvelet denoising.

So far, curvelets have been applied successfully for image denoising [30], image contrast enhancement [31], fusion of satellite images [9], motion estimation and video tracking [22], and surface characterization [21], among lots of literature. In [10], the adaptability of the curvelet transform for different tasks of computer vision like image retrieval, texture analysis and object recognition has been studied. Recently, Ma and Plonka presented two different models for image denoising by combining the curvelets with nonlinear diffusion schemes. In the first model [26], a curvelet shrinkage is applied to noisy data, and the result is further processed by a projected TV diffusion in order to suppress pseudo-Gibbs artifacts. In the second model [29], a nonlinear reaction-diffusion equation is applied, where curvelet shrinkage is used for regularization of the diffusion process.

Let us shortly explain the last mentioned approach that shows very good performance for denoising of images with textures. The reaction-diffusion model proposed in [29] is of the form

$$\frac{\partial u}{\partial t} = \nabla \cdot (g(|\nabla(P_\sigma u)|) \nabla u) + \gamma(Su_0 - u)$$

with the original noisy image u_0 as initial condition and with homogeneous Neumann boundary conditions. Here, $g(|x|) = (1 + 2500x^2)^{-1}$ is the Perona-Malik diffusivity. Now we use a curvelet shrinkage as regularization operator P_σ in the diffusion term, $P_\sigma u = T^{-1}S_\sigma T(u)$. The reaction term $\gamma(Su_0 - u)$ in the model cares for enhancement of oriented textures. For the operator S we can again take a curvelet shrinkage or, as proposed in [29], a wave atom shrinkage. Fig. 5(a) shows a part of the noisy Barbara image. Fig. 5(b) is the denoising result using curvelet shrinkage with hard threshold, Fig. 5(c) shows the performance of the reaction-diffusion model.

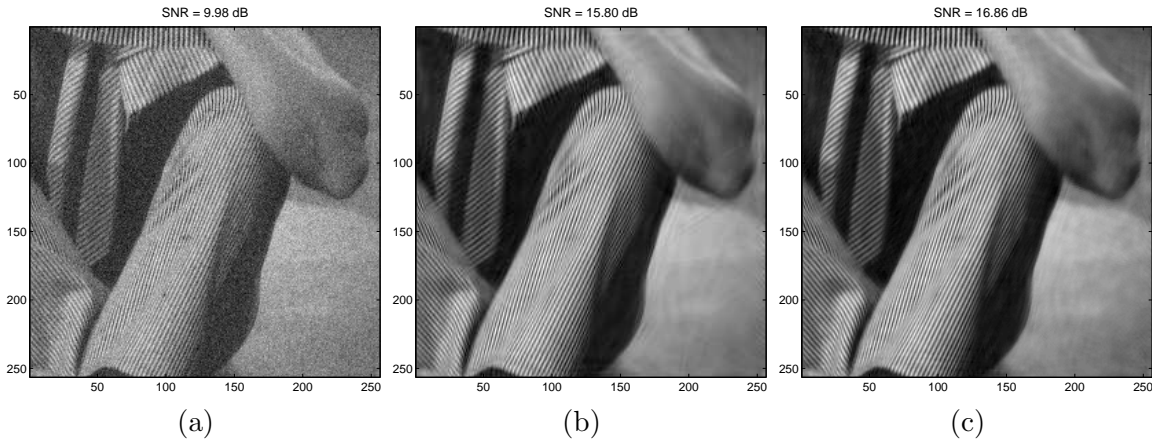


Figure 5: Image denoising. (a) noisy image. (b) curvelet denoising by hard thresholding. (c) denoising by curvelet regularized reaction-diffusion model.

5.2 Seismic exploration

Seismic data records amplitudes of reflecting waves during receiving time. The amplitude function of time is called seismic trace. A seismic data or profile is a collection of these traces. All the traces together provide a spatio-temporal sampling of reflected wave fields, which contain different arrivals that respond to different interactions of the incident wave field with inhomogeneities in the Earth’s subsurface. Common denominators among these arrivals are wave fronts (as shown in Fig. 6 (a) for a real seismic profile), which possess anisotropic line-like features, as edges and textures in images. They basically display behaviors of C^2 -continuous curves. The main characteristic of the wave fronts is their relative smoothness in the direction along the fronts and their oscillatory behavior in the normal direction. A crucial problem in seismic processing is to preserve the smoothness along the wave fronts when one aims to remove noise.

From a geophysical point of view, curvelets can be seen as local plane waves. They are optimal to sparsely represent the local seismic events and can be effectively used for wave front-preserving seismic processing. Now it is easy to understand why the curvelet decomposition is an appropriate tool for seismic data processing.

Fig. 6 shows a denoising example of a real seismic data with 512×512 size by wavelets, contourlets, and curvelets. It can be seen clearly that the curvelets perform much better than wavelets and contourlets to preserve the wave fronts/textures. The elapsed computation time of the curvelet, contourlet and wavelet denoising is 16.20s, 4.08s, and 1.47s using our laptop machine.

Hennenfent and Herrmann [17] suggested a nonuniformly sampled curvelet transform for seismic denoising. Neelamani et al. [27] proposed a 3D curvelet-based effective approach to attenuate random and coherent linear noise in a 3D data set from a carbonate environment. Douma and de Hoop presented a leading-order seismic imaging by curvelets [14]. Chauris and Nguyen [8] considered seismic demigration/migration in the curvelet domain. The migration consists of three steps: decomposition of the input seismic data (e.g., common offset sections) using the curvelet transform; independent migration of the curvelet coefficients; inverse curvelet transform to obtain the final depth migrated image. In addition, curvelet-based primary-multiple separation [19] and seismic data recovery [18] have been also proposed by Herrmann et al..

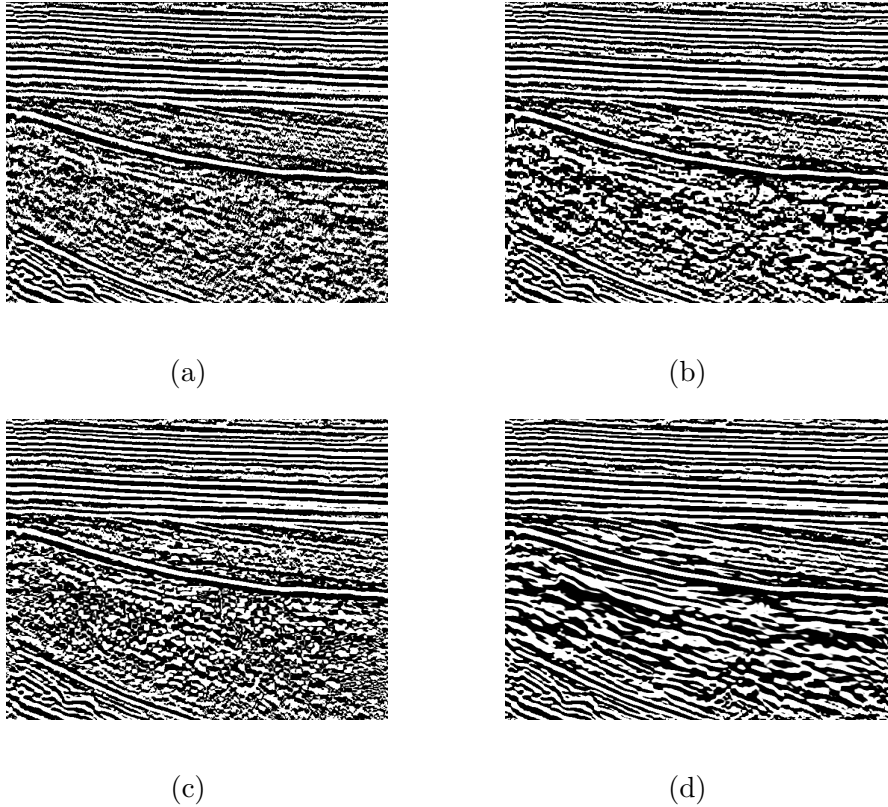


Figure 6: Comparison of seismic denoising. (a) original data. (b) wavelet denoising. (c) contourlet denoising. (d) curvelet denoising.

5.3 Turbulence analysis in fluid mechanics

Turbulence has been a source of fascination for centuries, because most fluid flows occurring in nature, as well as in engineering applications, are turbulent. Fluid turbulence is a paradigm of multiscale phenomena, where the coherent structures evolve in an incoherent random background. Turbulence is difficult to approximate and to analyze mathematically or to calculate numerically because of its range of spatial and temporal scales. The geometrical representation of flow structures might seem restricted to a well defined set of curves along which the data are singular. As a consequence, the efficient compression of a flow field with minimum loss of the geometric flow structures is a crucial problem in the simulation of turbulence. Development of appropriate tools to study vortex breakdown, vortex reconnection, turbulent entrainment at laminar-turbulent interfaces, is imperative to enhance our understanding of turbulence. Such tools must capture vortical structure and dynamics accurately to unravel the physical mechanisms underlying these phenomena.

Recently, the curvelets have been applied for a study of the non-local geometry of eddy structures and the extraction of the coherent vortex field in turbulent flows [1, 25]. Curvelets start to influence the field of turbulence analysis and have the potential to upstage the wavelet representations of turbulent flows addressed in e.g. [15]. The multiscale geometric properties, implemented by means of curvelets, provide the framework for studying the evolution of the structures as-

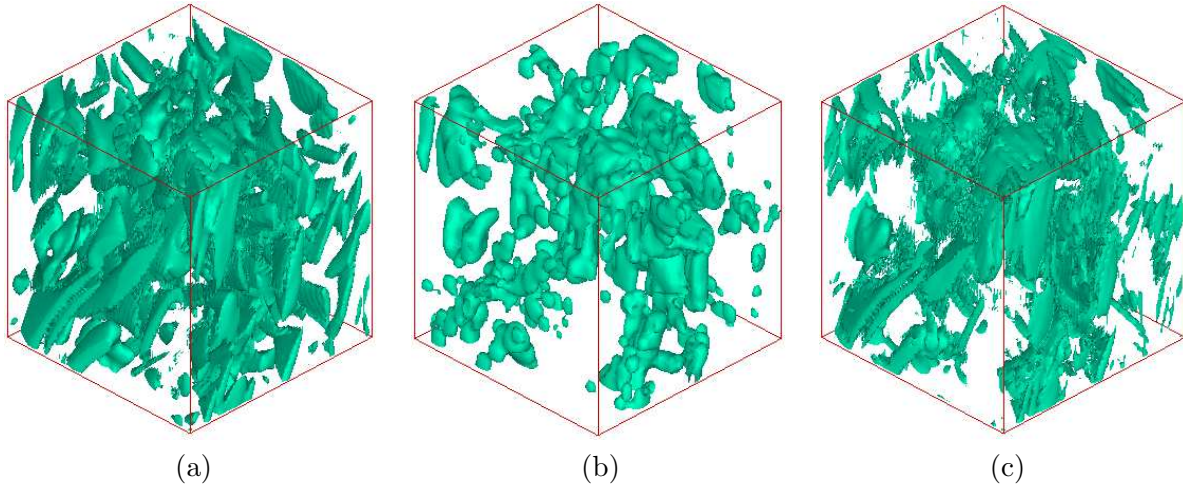


Figure 7: Extraction of coherent fields from turbulent flows. (a) Original flow. (b) Coherent components by wavelets. (c) by curvelets.

sociated to the main ranges of scales defined in Fourier space, while keeping the localization in physical space that enables a geometrical study of such structures. Such a geometrical characterization could provide improved understanding of cascade mechanics and dissipation-range dynamics. Moreover, curvelets have the potential to contribute to the development of structure-based models of turbulence fine scales, subgrid-scale models for large-eddy simulation, and simulation methods based on prior wavelet transforms [1].

In Fig. 7, we give an example for extraction of coherent fields from turbulent flows. The curvelet method preserves the edges and structures better than wavelet methods.

5.4 Compressed sensing

Finally, we mention a new direction of applications of the curvelet transform to the so-called compressed sensing or compressive sampling (CS), an inverse problem with highly incomplete measurements. CS [6, 7, 12] is a novel sampling paradigm, which carries imaging and compression simultaneously. It says that a compressible unknown signal can be recovered by a small number of random measurements using sparsity-promoting nonlinear recovery algorithms. The number of necessary measurements is considerably smaller than the number of needed traditional measurements that satisfy the Shannon/Nyquist sampling theorem, where the sampling rate has to be at least twice as large as the maximum frequency of the signals. The CS based data acquisition depends on its sparsity rather than its bandwidth. CS might have an important impact for design of measurement devices in various engineering fields such as medical magnetic resonance imaging and remote sensing, especially for cases involving incomplete and inaccurate measurements limited by physical constraints, or very expensive data acquisition.

Mathematically, we handle the fundamental problem of recovering a signal x from a small set of measurements y . Let A be a $K \times N$ measurement matrix of CS. Here $K \ll N$, i.e., there are much fewer rows in the matrix than columns. The measurement can be described as [6]

$$y = Ax + \epsilon. \quad (2)$$

Here ϵ denotes possible measurement errors or noise. Let K denote the number of measurements and N denotes the dimension of the signal x . It seems to be hopeless to solve the ill-posed underdetermined linear system since the number of equations is much smaller than the number of unknown variables. However, if the x is compressible by a transform, as e.g. $x = T^{-1}c$, where T denotes the discrete curvelet transform, and the sequence of discrete curvelet coefficients $c = (c_\mu)$ is sparse, then we have $Ty = TAT^{-1}c + \epsilon = \tilde{A}c + \epsilon$. If the measurement matrix A is noise-like incoherent/uncorrelated in the curvelet domain, the sparse sequence of curvelet coefficients c can be recovered by a sparsity-constraint l_1 -minimization [6],

$$\min_c \|Ty - \tilde{A}c\|_{l_2} + \lambda\|c\|_{l_1}.$$

The second term is a regularization term that represents the a-priori information of sparsity. To solve the minimization, an iterative curvelet thresholding can be used, based on the Landweber descent method,

$$c_{p+1} = S_\sigma(c_p + \tilde{A}^T(Ty - \tilde{A}c_p)),$$

until $\|c_{p+1} - c_p\| < \epsilon$, for a given error ϵ . The thresholding function S_σ can be taken as hard thresholding.

In Fig. 8, we show an example of compressed sensing with 25% Fourier measurements. Here the operator A is related to a Fourier transform followed by random subsampling. Fig. 8 (b) shows the samples in Fourier domain. Fig. 8 (c) is recovered by zero-filling reconstruction, and (d) is the result recovered by iterative curvelet thresholding.

The motivation of applying the curvelet thresholding method is that most natural images are compressible by the curvelet transform. Currently, a few researchers have applied the curvelet transform for compressed sensing in seismic data recovery [18] and remote sensing [23].

6 SOFTWARE OF CURVELETS

CurveLab is a collection of Matlab and C++ programs for the fast discrete curvelet transform in two and three dimensions. The latest version 2.1.2 (April 2008) is available from <http://www.curvelet.org>, made by Candès, Donoho, Demanet and Ying. There is a user's guide enclosed in the toolbox for installation guidelines. For questions and feedback, readers can reach them by curvelab@curvelet.org.

For the 2D curvelet transform, the software package includes two distinct implementations: the wrapping-based transform and the transform using unequally-spaced fast Fourier transform (USFFT).

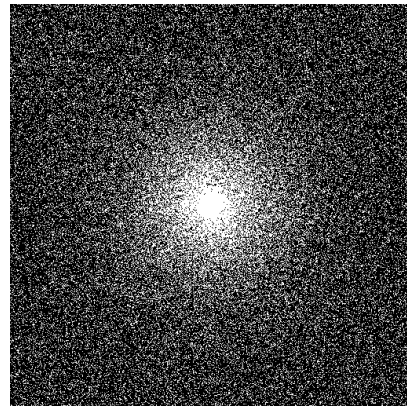
The USFFT version uses a decimated rectangular grid tilted along the main direction of each curvelet. There is one such grid per scale and angle, and this implementation is therefore very close to the definition of the discrete curvelet transform in [2], but has to use a resampling of the Fourier transform on semiregular grids. The wrapping version uses, instead, a decimated rectangular grid aligned with the image axes. The resulting sampling is not as faithful to the original transform, but does not need an interpolation in the frequency plane.

As to current stage, the wrapping algorithm is faster. Moreover, one can use curvelet elements in the finest scale, while in the USFFT algorithm one has to use the wavelets instead of curvelets in the finest scale. The redundancy of the curvelet transform implementation is about 2.8 when wavelets are chosen at the finest scale, and 7.2 otherwise (see e.g. [2]).



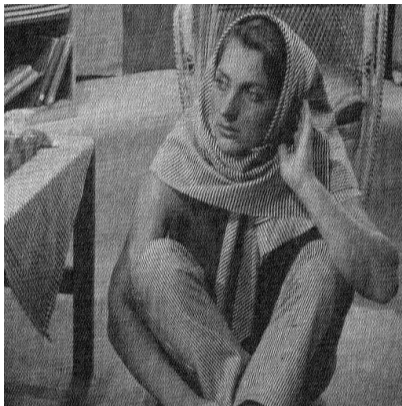
(a)

SNR = 29.15 dB



(b)

SNR = 44.46 dB



(c)



(d)

Figure 8: Compressed sensing in Fourier domain. (a) original Barbara image. (b) random Fourier sampling. (c) recovery by zero-filling reconstruction. (d) recovery by iterative curvelet thresholding.

For the 3D curvelet transform, the software in this package is an extension of the wrapping version in 2D. Due to the large size of the 3D data and the increasing redundancy of the curvelet transform, three different implementations involving memory-saving storage and parallel computation are provided.

The C++ part of the package includes all the 2D and 3D implementations. The Matlab part of this package includes only the 2D implementations of the USFFT and wrapping transforms. The C++ implementation works on Unix-type platforms including Linux, SunOS and MacOS. The Matlab code can work on Windows and Unix-type platforms.

7 FUTURE WORK

- 1) The computational cost of curvelets is higher than that of wavelets, especially in terms of 3D problems. However, the theory and application of the three-dimensional curvelets are burgeoning areas of research, and it is possible that more efficient curvelet-like transforms will be developed in the near future. Currently, a fast message passing interface-based parallel implementation can somewhat reduce the cost [33]. How to build a fast orthogonal curvelet transform is still open.
- 2) Currently, the curvelets are constructed in Fourier domain. There is no explicit space-domain formulation for curvelets. This brings troubles in many applications such as numerical modeling of PDEs. How to build a space-domain formulation of curvelets remains a challenge.
- 3) How to explore suitable thresholding functions that incorporate special directional characteristics of the curvelet transform is another crucial issue, which is important for edge detection, denoising, and numerical simulation in many engineering fields.

8 ACKNOWLEDGEMENTS

The authors would like to thank the Editor, Muhammad Sahimi, for his invitation to write this review. J. Ma has been supported by NSFC under Grant No. 40704019, TBRF (JC2007030), PetroChina Innovation Fund (060511-1-1). G. Plonka has been supported by the German Research Foundation within the project PL 170/13-1. These are grateful acknowledged.

References

- [1] I. Bermejo-Moreno, D. Pullin, On the non-local geometry of turbulence, *J. Fluid mech.*, **603**, 101-135 (2008).
- [2] E. Candès, L. Demanet, D. Donoho, L. Ying, Fast discrete curvelet transforms, *Multiscale Model. Simul.*, **5** (3), 861-899 (2006).
- [3] E. Candès, D. Donoho, Ridgelets: A key to higher-dimensional intermittency?, *R. Soc. Lond. Philos. Trans. Ser. A*, **357**, 2495-2509 (1999).
- [4] E. Candès, D. Donoho, Curvelets - a surprisingly effective nonadaptive representation for objects with edges, In *Curves and Surface Fitting: Saint-Malo 1999*, A. Cohen, C. Rabut, L. Schumaker (Eds.), Vanderbilt Univ. Press, Nashville, 2000, 105-120.
- [5] E. Candès, D. Donoho, New tight frames of curvelets and optimal representations of objects with piecewise singularities, *Comm. Pure Appl. Math.*, **57**, 219-266 (2004).
- [6] E. Candès, J. Romberg, T. Tao, Stable signal recovery from incomplete and inaccurate information, *Commun. Pure Appl. Math.*, **59**, 1207-1233 (2005).
- [7] E. Candès, T. Tao, Decoding by linear programming, *IEEE Trans. Infor. Theory*, **51**, 4203-4215 (2005).
- [8] H. Chauris, T. Nguyen, Seismic demigration/migration in the curvelet domain, *Geophysics*, **73** (2), S35-S46 (2008).
- [9] M. Choi, R. Kim, M. Nam, H. Kim, Fusion of multispectral and panchromatic satellite images using the curvelet transform, *IEEE Geosci. Remote Sensing Lett.*, **2** (2), 136-140 (2005).
- [10] S. Dekel, A. Sherman, Curvelets: a low-level framework for computer vision, preprint, GE Healthcare, 2008.

- [11] M. Do, M. Vetterli, The contourlet transform: an efficient directional multiresolution image representation, *IEEE Trans. Image Process.*, **14** (12), 2091-2106 (2005).
- [12] D. Donoho, Compressed sensing, *IEEE Trans. Inform. Theory*, **52** (4), 1289-1306 (2006).
- [13] D. Donoho, Wedgelets: nearly minimax estimation of edges, *Ann. Statistics*, **27** (3), 859-897 (1999).
- [14] H. Douma, M. de Hoop, Leading-order seismic imaging using curvelets, *Geophysics*, **72** (6), S231-S248 (2007).
- [15] M. Farge, N. Kevlahan, V. Perrier, E. Goirand, Wavelets and turbulence, *Proceedings of the IEEE*, **84** (4), 639-669 (1996).
- [16] K. Guo, D. Labate, Optimally sparse multidimensional representation using shearlets, *SIAM J. Math. Anal.*, **39**, 298-318 (2007).
- [17] G. Hennenfent, F. Herrmann, Seismic denoising with nonuniformly sampled curvelets, *Comput. Sci. Eng.*, **8** (3), 16-25 (2006).
- [18] F. Herrmann, P. Moghaddam, C. Stolk, Sparsity- and continuity-promoting seismic image recovery with curvelet frames, *Appl. Comput. Harm. Anal.*, **24** (2), 150-173 (2008).
- [19] F. Herrmann, D. Wang, D. Verschuur, Adaptive curvelet-domain primary-multiple separation, *Geophysics*, **73** (3), A17-A21 (2008).
- [20] N. Kingsbury, Image processing with complex wavelets, *Phil. Trans. R. Soc. Lond. A*, **357**, 2543-2560 (1999).
- [21] J. Ma, Curvelets for surface characterization, *Appl. Phys. Lett.*, **9**, 054109:1-3 (2007).
- [22] J. Ma, A. Antoniadis, F.-X. Le Dimet, Curvelets-based multiscale detection and tracking for geophysical fluids, *IEEE Trans. Geosci. Remote Sensing*, **44** (12), 3626-3637 (2006).
- [23] J. Ma, F.-X. Le Dimet, Deblurring from highly incomplete measurements for remote sensing, *IEEE Trans. Geosci. Remote Sensing*, 2008, to appear.
- [24] J. Ma, M. Fenn, Combined complex ridgelet shrinkage and total variation minimization, *SIAM J. Sci. Comput.*, **28** (3), 984-1000 (2006).
- [25] J. Ma, M. Hussaini, Three-dimensional curvelets for coherent vortex analysis of turbulence, *Appl. Phys. Lett.*, **91**, 184101:1-3 (2007).
- [26] J. Ma, G. Plonka, Combined curvelet shrinkage and nonlinear anisotropic diffusion, *IEEE Trans. Image Process.*, **16** (9), 2198-2206 (2007).
- [27] R. Neelamani, A. Baumstein, D. Gillard, M. Hadidi, W. Soroka, Coherent and random noise attenuation using the curvelet transform, *The Leading Edge*, **27** (2), 240C248 (2008).
- [28] E. Le Pennec, S. Mallat, Sparse geometrical image approximation with bandlets, *IEEE Trans. Image Process.*, **14** (4), 423-438 (2005).
- [29] G. Plonka, J. Ma, Nonlinear regularized reaction-diffusion filters for denoising of images with textures, *IEEE Trans. Image Process.*, **17** (8), 1283-1294 (2008).
- [30] J. Starck, E. Candès, D. Donoho, The curvelet transform for image denoising, *IEEE Trans. Image Process.*, **11**, 670-684 (2002).
- [31] J. Starck, F. Murtagh, E. Candès, F. Murtagh, D. Donoho, Gray and color image contrast enhancement by the curvelet transform, *IEEE Trans. Image Process.*, **12** (6), 706-717 (2003).
- [32] R. Willett, K. Nowak, Platelets: A multiscale approach for recovering edges and surfaces in photon-limited medical imaging, *IEEE Trans. Med. Img.*, **22** (3), 332-350 (2003).
- [33] L. Ying, L. Demanet, E. Candès, 3D Discrete Curvelet Transform, *Proc. of SPIE Wavelets XI*, Vol. 5914, 591413, San Diego, CA, 2005.